

Stellar collisions in globular clusters: constraints on the IMF of the first generation of stars

Sami Dib¹, Valery V. Kravtsov², Hosein Haghi³, Akram Hasani Zonoozi³, José Antonio Belinchón⁴

¹ Max Planck Institute for Astronomy, Königstuhl 17, 69117, Heidelberg, Germany
e-mail: sami.dib@gmail.com; dib@mpia.de

² Sternberg Astronomical Institute, Lomonosov Moscow State University, University Avenue 13, 119899 Moscow, Russia

³ Department of Physics, Institute for Advanced Studies in Basic Sciences (IASBS), Zanjan 45137-66731, Iran

⁴ Departamento de Matemáticas, Universidad de Atacama, Av. Copayapu 485, Copiapó, Chile

March 23, 2022

ABSTRACT

Globular clusters display an anti-correlation between the fraction of the first generation of stars ($N(G1)/N(\text{tot})$) and the slope of the present-day mass function of the clusters (α_{pd}), which is particularly significant for massive clusters. In the framework of the binary-mediated collision scenario for the formation of the second generation stars in globular clusters, we test the effect of a varying initial stellar mass function (IMF) of the G1 stars on the $(N(G1)/N(\text{tot})) - \alpha_{pd}$ anti-correlation. We use a simple collision model which has only two inputs, the IMF of G1 stars and the fraction of G1 stars that coalesce to form G2 stars. We show that a variable efficiency of the collision process is necessary in order to explain the $(N(G1)/N(\text{tot})) - \alpha_{pd}$ anti-correlation, however, the scatter in the anti-correlation can only be explained by variations in the IMF, and in particular by variations of the slope in the mass interval $\approx (0.1-0.5) M_{\odot}$. Our results indicate that in order to explain the scatter in the $(N(G1)/N(\text{tot})) - \alpha_{pd}$ relation, it is necessary to invoke variations of the slope in this mass range between ≈ -0.9 and ≈ -1.9 . Interpreted in terms of a Kroupa-like broken power law, this translates into variations of the mean mass between ≈ 0.2 and $0.55 M_{\odot}$. This level of variations is consistent with what is observed for young stellar clusters in the Milky Way and may reflect variations in the physical conditions of the globular clusters progenitor clouds at the time the G1 population has formed or to the occurrence of collisions between protostellar embryos before stars settle on the Main Sequence.

Key words. stars: formation - ISM: clouds, general, structure - galaxies: ISM, star formation

1. Introduction

The stellar initial mass function (IMF) of stars (i.e., the distribution of the masses of stars at their birth), is of fundamental importance in astrophysics. The IMF controls the efficiency of star formation in molecular clouds (Dib et al. 2011, 2013; Hony et al. 2015), the radiative and mechanical feedback from stars into the large scale interstellar medium (Dib et al. 2006, 2021; Martizzi et al. 2016; Silich & Tenorio-Tagle 2017) and the dynamical and chemical evolution of galaxies (Côté et al. 2016). Significant efforts have been devoted to the determination of the shape of the IMF in a variety of environments, from the Galactic field (Salpeter 1955; Bochanski et al. 2010; Rybizki & Just 2015; Mor et al. 2019; Sollima 2019), the Galactic bulge (Wegg et al. 2017) and in galactic open clusters both old and young (Dib 2014; Weisz et al. 2015; Maia et al. 2016; Dib et al. 2017; Jose et al. 2017; Madaan et al. 2020; Bisht et al. 2021; Damian et al. 2021; Elsanhoury et al. 2022). In the galactic ecosystem, globular clusters (GCs) stand out as relics of early star formation (Pfeffer et al. 2018) and it is well established that GCs in the Milky Way and in the Magellanic clouds harbor two or more stellar populations (d’Antona & Caloi 2008; Milone et al. 2010; Sbordone et al. 2011; Gratton et al. 2012; Cummings et al. 2014; Piotto et al. 2015; Lee 2015; Oldham & Auger 2016; Mucciarelli et al. 2016; Massari et al. 2016; Dalessandro et al. 2016; Bowman et al. 2017; Carretta & Bragaglia 2018; Latour et al. 2019;

Gilligan et al. 2020; Dondoglio et al. 2021; Jang et al. 2021; D’Antona et al. 2022; Kapse et al. 2022).

The origin of the multiple stellar populations in globular clusters is highly debated. A number of scenarios have been proposed in order to explain the existence of two or more stellar populations. The oldest and most popular of these is the AGB self-enrichment scenario which is based on the formation of second generation stars (hereafter G2 stars) from the ejecta of the first generation (G1) AGB stars after gas has been cleared from the cluster by feedback from massive stars (Cottrell & Da Costa 1981; D’Ercole et al. 2016; Bekki 2017). Since the pure AGB scenario fails to reproduce the observed Na-O anticorrelation, a modified version of the model was introduced whereby pristine gas is accreted from outside the cluster and mixes with the AGB ejecta to form the G2 stars (Ventura & D’Antona 2009; Calura et al. 2019; Yaghoobi et al. 2022). Other variants of the model relied on the ejecta of fast rotating massive stars (FRMS) instead of AGB stars (Decressin et al. 2007; Krause et al. 2013) or on the rapid efficient cooling of stellar winds material which falls back to the centre of the cluster and mixes with leftover gas with a G1-like chemical composition (Wünsch et al. 2017). Other models invoked a dichotomy in GC mass whereby the efficiency of the AGB ejecta retention in the cluster would depend on the cluster mass (Valcarce & Catelan 2011). The AGB- and the FRMS-based scenarios suffer from the same type of shortcomings. It is unclear whether the AGB (or FRMS) stars gas ejecta can cool and form the second generation of stars due to

uninterrupted heating by G1 stars, particularly from X-ray binaries that heat the gas and prevent it from fragmenting (Conroy & Spergel 2011). Another issue is the so-called mass-budget problem. This problem reflects the inability of G1 stars, under the assumption of a Milky Way like IMF, to produce enough chemically enriched material for the formation of a significant populations of G2 stars. Furthermore, and owing to the GCs orbits in the galaxy, it is not clear whether accretion of external gas would be efficient (Conroy & Spergel 2011). Khalaj & Baumgardt (2015) investigated under which conditions the loss of G1 stars due to gas expulsion from the protocluster cloud can help reproduce the fraction of G2 stars and some of the clusters properties such as their radial profiles and mass-half mass-radius relation. They found that reproducing the observations requires rapid gas expulsion timescales ($\lesssim 10^5$ yr) and a large number of supernovae explosions, which is 3-6 times higher than what would be found in a Galactic field-like IMF.

Another physical process that can lead to the formation of a significant fraction of G2 stars over a short timescale, prior to gas expulsion from the clusters by the first supernovae is stellar collisions (Sills et al. 2002; Sills & Glebbeek 2010; Jiang et al. 2014; Wang et al. 2020; Kravtsov & Calderón 2021; Kravtsov et al. 2022). Collisions not only set the relative fractions of the first and second generations stars but they also alter the shape of the IMF of the G1 stars (Dib et al. 2007; Kravtsov et al. 2022). While more work is still needed in order to understand whether stellar collisions, particularly of low mass stars, can lead to the chemical anti-correlations that are observed for GCs, Kravtsov et al. (2022) presented observational evidence that support the scenario in which stellar collisions of G1 stars in the mass range $\approx (0.1-0.5) M_\odot$ can lead to the formation of G2 stars in the mass range $(0.5-0.9) M_\odot$. In particular, evidence was presented for the existence of an anti-correlation between the fraction of G1 stars ($N(\text{G1})/N(\text{tot})$) and the slope of the present-day mass function of GCs in the stellar mass range $(0.2-0.8) M_\odot$ (α_{pd}). They also found that the fraction of G1 stars is anti-correlated with the encounter rate measured in these clusters. Using a simple collision model with a parametrized collision efficiency and a Kroupa-like IMF for the G1 stars, Kravtsov et al. (2022) showed that it is possible to reproduce the $(N(\text{G1})/N(\text{tot})) - \alpha_{pd}$ anti-correlation both in terms of slope and absolute values. Nonetheless, the $(N(\text{G1})/N(\text{tot})) - \alpha_{pd}$ anti-correlation shows a level of scatter that cannot be simply explained by a fixed IMF nor by observational uncertainties. In this paper, and in the framework of this-collision based scenario, we focus on the role of the IMF in explaining both the trend and scatter in the $(N(\text{G1})/N(\text{tot})) - \alpha_{pd}$ relation. In particular, we explore how variations in the shape of the IMF can impact the shape of the $(N(\text{G1})/N(\text{tot})) - \alpha_{pd}$ anti-correlation. In §. 2 and §. 3 we briefly recall the observational data and the main elements of the model that is used to reproduce them, respectively. The results are presented in §. 4, and in §. 5, we conclude.

2. Data

We use the sample on multiple stellar populations in Galactic GCs obtained by Milone et al. (2017). Using uniform multiband HST photometry (Sarajedini et al. 2007; Piotto et al. 2015) in the central parts of a sample of 57 GCs. Milone et al. (2017) isolated Red Giant Branch (RGB) stars and measured the fractions of the G1 population to the total number of RGB stars ($N(\text{G1})/N(\text{tot})$). These fractions were measured for a total of 54 GCs. For the slope of the present-day mass function, we use the compilation of Ebrahimi et al. (2020) which includes 32 GCs and for which

the slope has been measured by fitting a power-law in the stellar mass range $(0.2-0.8) M_\odot$. The cluster NGC 6584 was excluded from our sample since the data on this GC is incomplete. The data for four additional GCs was taken from Sollima & Baumgardt (2017), namely NGC 4833, NGC 6205, NGC 6397, and NGC 6656 and the measurement of α_{pd} for those clusters was also performed by fitting a single power law over the same stellar mass range of $(0.2-0.8) M_\odot$. In total, we have a sample of 35 GCs with measurements of $(N(\text{G1})/N(\text{tot}))$ and α_{pd} .

3. Model

In the framework of the collision-based scenario, our aim is to understand the effect of the shape of the IMF of the G1 stars on the observed $(N(\text{G1})/N(\text{tot})) - \alpha_{pd}$ anti-correlation. Understanding the precise effects of collisions requires calculating the collision rates over the entire stellar mass range and a knowledge of the coalescence efficiency as a function of stellar mass (e.g., Dib et al. 2007). Here, we use a simpler model with two mass bins, similar to the one used in Kravtsov et al. (2022). We briefly recall its basic elements. We assume that stars that can coalesce are those exclusively found in the stellar mass range $(0.1-0.5) M_\odot$. The collision products (G2 stars) are more massive stars with masses that fall in the range $(0.5-0.9) M_\odot$. If $N_1(\text{G1})$ and $N_2(\text{G1})$ are the total numbers of G1 stars that fall in the target and product mass bins, respectively, then the fractions of these two population of stars to the total number of stars (N'_{tot}) can be written as:

$$f_{1,in} = \frac{N_1(\text{G1})}{N'_{tot}}, \quad (1)$$

and

$$f_{2,in} = \frac{N_2(\text{G1})}{N'_{tot}}. \quad (2)$$

If $N_{1,ext}(\text{G1}) = f_{ext}N_1(\text{G1})$ is the total number of stars that have experienced a collision and under the assumption that we can only have two stars colliding to form a new one and with f_{ext} being the fraction of $N_1(\text{G1})$ stars that undergo a collision, then, the new number of stars becomes:

$$N_{tot} = N'_{tot} - \frac{f_{ext}N_1(\text{G1})}{2}. \quad (3)$$

After the collision process, a second generation of stars is formed in the mass range $(0.5-0.9) M_\odot$ (i.e., G2 stars). The new fractions of stars in the above mentioned mass ranges will be given by:

$$f_{1,fl} = \frac{N_1(\text{G1}) - f_{ext}N_1(\text{G1})}{N_{tot}} = \frac{2f_{1,in}(1 - f_{ext})}{2 - (f_{ext}f_{1,in})}, \quad (4)$$

and

$$f_{2,fl} = \frac{N_2(\text{G1}) + f_{ext}N_1(\text{G1})/2}{N_{tot}} = \frac{2f_{2,in} + f_{ext}f_{1,in}}{2 - (f_{ext}f_{1,in})}. \quad (5)$$

The value of $(N(\text{G1})/N(\text{tot}))$ for RGB stars is given by its analog for MS stars as:

$$g_1 = \frac{N_2(\text{G1})}{N_2(\text{G1}) + N_2(\text{G2})} = \frac{2f_{2,in}}{2f_{2,in} + f_{ext}f_{1,in}}. \quad (6)$$

For the globular clusters in our sample, we have access to $(N(\text{G1})/N(\text{tot}))$ and α_{pd} . Assuming that the effects of dynamical evolution are negligible in the stellar mass range $[0.2, 0.8] M_\odot$ over which the values of α_{pd} are measured, these values of α_{pd} would reflect the effects of the stellar collision process. In the model, and for any given functional form of the IMF, we can measure the values of $f_{1,in}$, $f_{2,in}$, and for a given value of f_{ext} , we can calculate the values of $f_{1,fl}$, $f_{2,fl}$, and g_1 . With $f_{1,fl}$ and $f_{2,fl}$ we can also derive the value of the post-collision value of the slope, α_{pc} . We calculate the value of α_{pc} as being $\alpha_{pc} = (\log(f_{1,fl}) - \log(f_{2,fl})) / (\log(0.7) - \log(0.3))$, where 0.3 and 0.7 (in units of M_\odot) are the mean masses in the intervals $(0.1-0.5) M_\odot$ and $(0.5-0.9) M_\odot$, respectively. We note that the parameter g_1 for MS stars is formally equivalent to the ratio $(N(\text{G1})/N(\text{tot}))$ deduced from the observations of RGB stars. However, some caution should be exercised. As already noted in Kravtsov et al. (2022), the fractions $(N(\text{G1})/N(\text{tot}))$ have been measured in the central parts of GCs. Since RGB G2 stars are typically observed to be more centrally located than their G1 counterparts, the real $(N(\text{G1})/N(\text{tot}))$ fractions should be systematically higher than the values that are actually derived. In contrast, the parameter g_1 in the models is assumed to be measured for the clusters as a whole. Furthermore, g_1 is assumed to be a proxy for MS stars that are found now on the RGB. However, the observed fraction $(N(\text{G1})/N(\text{tot}))$ could also contain, in addition to RGB stars whose masses fall in the range $\approx (0.8-0.85) M_\odot$, a contribution from more massive blue straggler stars that are either of collisional origin or that have been formed by mass transfer in binaries. For the reasons discussed above, we prefer to formally distinguish between $(N(\text{G1})/N(\text{tot}))$ which is derived from the observations and g_1 which is calculated in the models, even if in practice the two quantities are expected to be very close.

4. Results

We describe the IMF of the G1 stars using a multi-component power-law function which is given by (Kroupa 2001):

$$\psi(M) = A \begin{cases} \left(\frac{M}{0.08}\right)^{\alpha_0}, & M \leq 0.08 M_\odot \\ \left(\frac{M}{0.08}\right)^{\alpha_1}, & 0.08 M_\odot \leq M \leq 0.5 M_\odot \\ \left(\frac{0.5}{0.08}\right)^{\alpha_1} \left(\frac{M}{0.5}\right)^{\alpha_2}, & M \geq 0.5 M_\odot, \end{cases} \quad (7)$$

and where A is a normalization constant that depends on the cluster mass. Its determination is not necessary since we are only interested in the fractions of stars in the target and product mass bins. When calculating the fractions, we assume that the minimum and maximum stellar masses are $M_{min} = 0.01 M_\odot$ and $M_{max} = 150 M_\odot$, respectively. In Eq. 7, the value of α_0 is the most uncertain and displays a significant amount of scatter amongst the Milky Way clusters. We fix its value to the one derived for the Galactic field, namely $\alpha_0 = -0.3$. In the first instance, we consider the effect of varying the value of the slope at the high mass end, α_2 . The Galactic field value is ≈ -2.3 , and we consider here a range of values going from -1.7 to -2.7 . The value of α_1 is set to Galactic field value of -1.3 . The shape of the IMF for various values of α_2 , for the same arbitrary mass reservoir, is displayed in Fig. 1. For each set of free parameters (α_2 and f_{ext}), we calculate the values α_{pc} and g_1 using the model described in § 3. The results in the $g_1 - \alpha_{pc}$ space are displayed in Fig. 2 and are compared to the observational data. Variations in α_2 , coupled to variations of f_{ext} in the range (0.2-0.6) can help explain a fraction of the scatter that is observed in

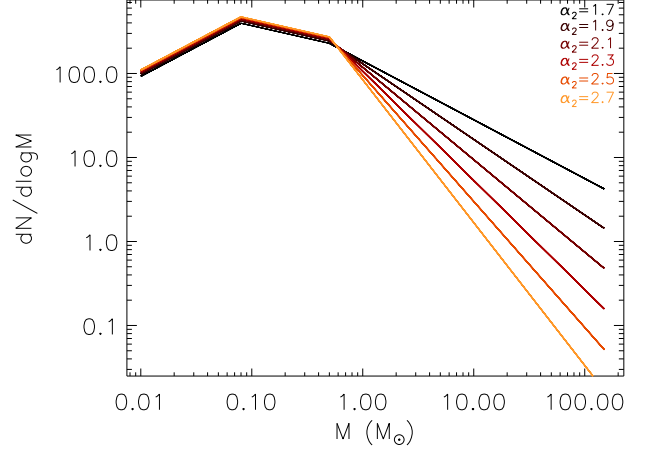


Fig. 1. Shape of the IMF for various values of the slope at the high mass end, α_2 , around the Galactic field value of -2.3 . The values of α_0 and α_1 are set to the Galactic field values of -0.3 and -1.3 , respectively. The mass functions are normalized assuming the same arbitrary mass.

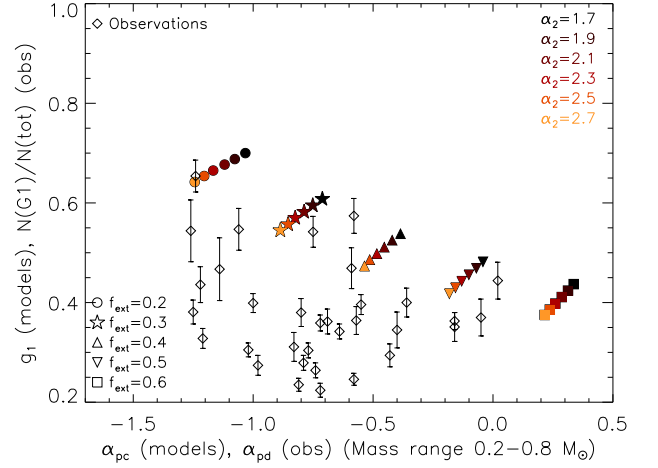


Fig. 2. The relationship between g_1 and the slope of the post-collision mass function, α_{pc} (for stars in the mass range $0.2-0.8 M_\odot$), for various shapes of the IMF, namely for various values of the slope at the high mass range, α_2 , and for various values of f_{ext} . In all models, the values of α_0 and α_1 are fixed to -0.3 and -1.3 , respectively. The models are compared to the $(N(\text{G1})/N(\text{tot})) - \alpha_{pd}$ relation found in the observations.

the $(N(\text{G1})/N(\text{tot})) - \alpha_{pd}$ relation but fall short of explaining the values of $(N(\text{G1})/N(\text{tot}))$ that are $\lesssim 0.4$.

It is evident that variations in $(N(\text{G1})/N(\text{tot}))$ (equivalently in g_1 for the models) would be more significant if the primordial fractions of G1 stars were different, as a consequence of variations in the physical conditions of the star formation process. Dib (2014) and Dib et al. (2017) showed that the characteristic mass (i.e., the peak of the IMF when fitted with a tapered power-law function) varies in the range of ≈ 0.1 to $\approx 0.8 M_\odot$ when measured for young clusters in the Milky Way. It is not clear whether the same level of variations is present in the IMF of GCs at the time they formed. Since we are using a broken power law function with no well defined peak, we vary the intermediate slope of the IMF in the mass range $(0.08-0.5) M_\odot$ (i.e., α_1). Figure 3

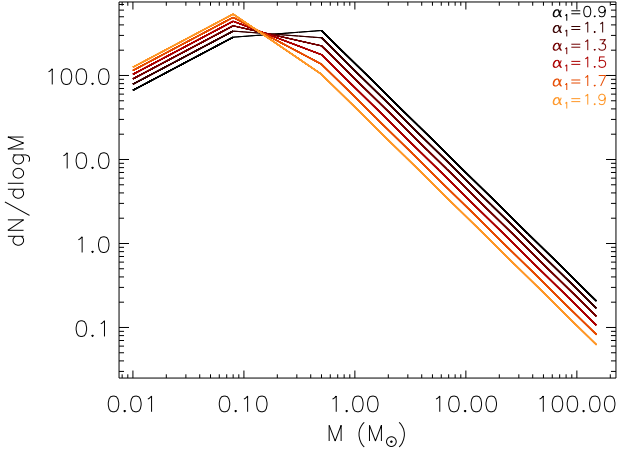


Fig. 3. Shape of the IMF for various values of the intermediate slope, α_1 , around the Galactic field value of -1.3 . The values of α_0 and α_2 are set to the Galactic field values of -0.3 and -2.3 , respectively. The mass functions are normalized assuming the same arbitrary mass.

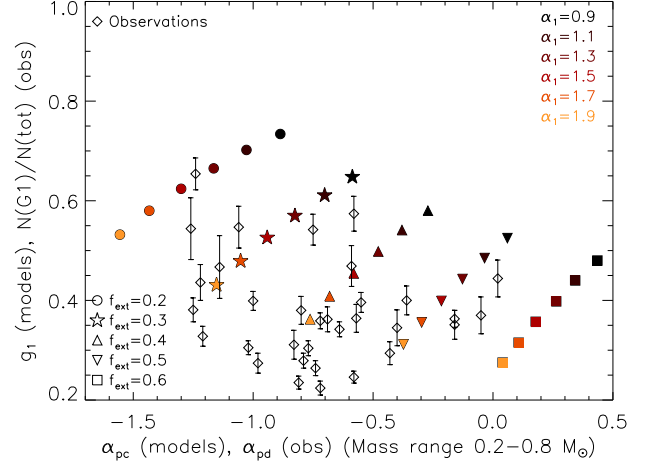


Fig. 4. The relationship between g_1 and the slope of the post collision mass function, α_{pc} (for stars in the mass range $0.2-0.8 M_\odot$), for various shapes of the IMF, namely for various values of the slope in the intermediate mass range, α_1 , and for various values of f_{ext} . In all models, the values of α_0 and α_2 are fixed to -0.3 and -2.3 , respectively. The models are compared to the $(N(G1)/N(tot)) - \alpha_{pd}$ found in the observations.

displays a numbers of IMF realizations for various values of α_1 and where α_0 and α_2 are assigned the Galactic field values of -0.3 and -2.3 , respectively. The derived $g_1 - \alpha_{pc}$ relations for these different cases and for various values of f_{ext} are displayed in Fig. 4. As already shown in Kravtsov et al. (2022), varying the value of f_{ext} for a fixed set of the IMF parameters reproduces the anti-correlation between $(N(G1)/N(tot)) - \alpha_{pd}$. However, in order to reproduce the observed level of scatter in the observations, it is necessary to allow, for a fixed value of f_{ext} , the existence of variations in the values of α_1 . This level of variations in α_1 translates into a mean mass that varies between 0.2 and $0.55 M_\odot$. This level of variations is consistent with what is observed for young stellar clusters in the Milky Way (Dib 2014; Dib et al. 2017). Keeping in mind that the true values of $(N(G1)/N(tot))$ could be systematically higher than the observed ones, the simple models presented here reproduce the observations remarkably well. It is also worth pointing out that variations in α_1 and α_2 can occur simultaneously. Furthermore, we have restricted the distinct power laws to mass ranges similar to those inferred for the Galactic field. There is however no indication that these limits hold for individual clusters and that they may well vary from cluster to cluster as is observed in young clusters in the Milky Way (Dib 2014).

5. Discussion and conclusions

In this work, we explore in globular clusters that harbor multiple populations, the origin of the anti-correlation that is observed between the fraction of the first generation of stars $(N(G1)/N(tot))$ and the slope of the present-day mass function of the clusters in the stellar mass range $(0.2-0.8 M_\odot)$ (α_{pd}). We compare the observation to a simple model which is based on the idea of stellar collisions between first generation stars in the mass range $(0.1-0.5 M_\odot)$ that lead to the formation of a second generation of stars with masses in the range of $(0.5-0.9 M_\odot)$. The model has two main inputs which are the IMF of the G1 stars and the fraction of G1 stars in the $(0.1-0.5 M_\odot)$ mass range that collide to form G2 stars (parameter f_{ext}). The parameter f_{ext} encapsulates much of the physics that governs the efficiency of the collision process.

Its value would depend on the compactness of the protocluster cloud, and hence on the mean distance between stars and also on other factors such as the initial levels of mass segregation in the clusters, the binary fraction, and the period distribution of binaries, among other quantities. We find that the appropriate range for f_{ext} is $\approx (0.2 - 0.6)$. Smaller values and larger values lead to values of the slope that are outside the range of observed values.

Our results show that variations in f_{ext} are necessary in order to explain the anti-correlation between $(N(G1)/N(tot))$ and α_{pd} for a fixed shape of the IMF. However, the large scatter that is observed in the $(N(G1)/N(tot)) - \alpha_{pd}$ anti-correlation can only be explained, in the framework of this collision-based model, by variations in the IMF of the G1 stars. In particular, we show that variations of the slope of the IMF in the intermediate mass regime of a Kroupa-like IMF ($\approx 0.08 - 0.5$) in the range -1.9 to -0.9 can reproduce the scatter in $(N(G1)/N(tot))$ at a given value of α_{pd} . This level of variations in α_1 corresponds to a range of $\approx (0.2-0.55 M_\odot)$ in the mean stellar mass in the clusters. In this work, we have restricted the target G1 stars to the mass range $(0.1-0.5 M_\odot)$. However, merger between stars whose stars fall in the range $(0.1-0.9 M_\odot)$ and that result in G2 stars with masses $\leq 0.9 M_\odot$ can further decrease the ratio $(N(G1)/N(tot))$ and bring the model into a better agreement with the observations. Variations of the IMF of GCs have been pointed out by other groups. Zonoozi et al. (2016) showed that a dependence of the high mass end of the IMF on metallicity as proposed by Marks & Kroupa (2012) can help explain the mass-to-light vs. metallicity anti-correlation that is observed for the population of GCs in M31.

It is useful to point out that de Marchi et al. (2010) fitted the present-day mass function of many Galactic clusters, young and old, with a tapered power-law function and deduced that the characteristic mass varies between 0.1 to $0.8 M_\odot$ which is roughly the same range of variations implied by our model. However, de Marchi et al. attributed the difference in the characteristic mass to the preferential evaporation of low mass stars from the clusters, leading over time to a shift of the characteristic mass to higher values. While it is probably safe to say that the jury is still out concerning the relative importance of collisions

versus dynamical interactions in modifying the shape of the IMF in GCs, the collision-based model presented here provides an explanation for the observed $(N(G1)/N(\text{tot})) - \alpha_{pd}$ anti-correlation and it is not yet clear if dynamical evolution can do the same. The level of variations of the IMF inferred in this work, particularly for the slope in the stellar mass range $(0.08-0.5) M_{\odot}$ that is needed in order to explain the scatter in the $(N(G1)/N(\text{tot})) - \alpha_{pd}$ relation is consistent with what is observed for young stellar clusters in the Milky Way (Dib 2014) and may reflect either variations in the physical conditions of the GCs parental clouds at the time the G1 population started to form or to the occurrence of other processes such as gas accretion onto protostars (Dib et al. 2010) or collisions between protostars before they settle on the Main Sequence (Dib et al 2007).

References

- Bekki, K., 2017, MNRAS, 467, 1857
 Bisht, D., Zhu, Q., Elsanhoury, W. H. et al. 2021, PASJ, 73, 677
 Bochanski, J. J. et al. 2010, AJ, 139, 2679
 Bowman, W. P. et al. 2017, AJ, 154, 131
 Calura, F. et al. 2019, MNRAS, 489, 3269
 Carretta, E., Bragaglia, A. 2018, A&A, 614, 109
 Conroy, C., Spergel, D. N. 2011, ApJ, 726, 36
 Côté, B., Ritter, C., O’Shea, B. W. et al. 2016, ApJ, 824, 82
 Cottrell, P. L., Da Costa, G. S. 1981, ApJ, 245, 79
 Cummings, J. D. et al. 2014, AJ, 148, 27
 D’Antona, F., Caloi, V. 2008, MNRAS, 390, 693
 D’Antona, F. et al. 2022, ApJ, 925, 192
 Dalessandro, E. et al. 2016, ApJ, 829, 77
 Damian, B., Jose, J., Samal, M. et al. 2021, MNRAS, 504, 2557
 Decressin, T., Charbonnel, C., Meynet, G. 2007, A&A, 475, 859
 De Marchi, G. et al. 2010, ApJ, 718, 105
 D’Ercole, A. et al. 2016, MNRAS, 461, 4088
 Dib, S., Bell, E., Burkert, A. 2006, ApJ, 638, 797
 Dib, S., Kim, J., Shadmehri, M. 2007, MNRAS, 381, L40
 Dib, S., Shadmehri, M., Padoan, P. et al. 2010, MNRAS, 405, 401
 Dib, S., Piau, L., Mohanty, S. et al. 2011, MNRAS, 415, 3439
 Dib, S., Gutkin, J., Brandner, W. et al. 2013, MNRAS, 436, 3727
 Dib, S. 2014, MNRAS, 444, 1957
 Dib, S., Schmeja, S., Hony, S. 2017, MNRAS, 464, 4018
 Dib, S., Braine, J., Maheswar, G. et al. 2021, A&A, 655, 101
 Dondoglio, E., Milone, A. P., Lagioia, E. P. et al. 2021, 906, 76
 Ebrahimi, H. et al. 2020, MNRAS, 494, 4226
 Elsanhoury, W. H. et al. 2022, JAA, arXiv:2201.04015
 Gilligan, C. K. et al. 2020, MNRAS, 494, 1946
 Gratton, R. G., Carretta, E., Bragaglia, A. 2012, A&ARv, 20, 50
 Hony, S. et al. 2015, MNRAS, 448, 1847
 Jang, S., Milone, A. P., Lagioia, E. P. 2021, ApJ, 920, 121
 Jiang, D., Han, Z., Li, L. 2014, ApJ, 789, 88
 Jose, J., Herczeg, G. J., Samal, M. et al. 2017, ApJ, 836, 98
 Kapse, S., de Grijs, R., Kamath, D., Zucker, D. B. 2022, ApJ, 927, 10
 Krause, M., et al. 2013, A&A, 552, 121
 Kravtsov, V. V. et al. 2010, A&A, 512, 6
 Kravtsov, V. V. et al. 2014, A&A, 783, 56
 Kravtsov, V., & Calderón, F. A. 2021, AJ, 161, 7
 Kravtsov, V. V., Dib, S., Calderón, F. A., Belinchón, J. A. 2022, MNRAS, in press, arXiv:2203.02893
 Kroupa, P. 2001, MNRAS, 322, 231
 Latour, M., Husser, T.-O., Giesers, B. et al. 2019, A&A, 631, 14
 Lee, J.W. 2015, ApJS, 219, 7
 Madaan, D., Lianou, S., Basu, S. 2020, ApJ, 895, 66
 Maia, F. F. S., Moraux, E., Joncour, I. 2016, MNRAS, 458, 3027
 Marks, M. et al. 2012, MNRAS, 422, 2246
 Massari, D. et al. 2016, MNRAS, 458, 4162
 Milone, A. P., Piotto, G., King, I. R. et al. 2010, ApJ, 709, 1183
 Milone, A. P. et al. 2017, MNRAS, 464, 3636
 Mor, R., Robin, A. C., Figueras, F. et al. 2019, A&A, 624, 1
 Mucciarelli, A. et al. 2016, ApJ, 824, 73
 Oldham, L. J., Auger, M. W. 2016, MNRAS, 455, 820
 Piotto, G., Milone, A. P., Bedin, L. R. et al. 2015, AJ, 149, 91
 Pfeffer, J. et al. 2018, MNRAS, 475, 4309
 Rybizki, J., Just, A. 2015, MNRAS, 447, 3880
 Salpeter, E. E. 1955, ApJ, 121, 161
 Sarajedini, A. et al. 2007, AJ, 133, 1658
 Sbordone, L. et al. 2011, A&A, 534, 9
 Silich, S., Tenorio-Tagle, G. 2017, MNRAS, 465, 1375
 Sills, A., Adams, T., Davies, M. B. et al. 2002, MNRAS, 332, 49
 Sills, A., Glebbeek, E. 2010, 407, 277
 Sollima, A., Baumgardt, H. 2017, MNRAS, 471, 3668
 Sollima, A. 2019, MNRAS, 489, 2377
 Valcarce, A. A. R., Catelan, M. 2011, A&A, 533, 120
 Ventura, P., D’Antona, F. 2009, A&A, 499, 835
 Wang, L. et al. 2020, MNRAS, 491, 440
 Wegg, C., Gerhard, O., Portail, M. 2017, ApJ, 843, 5
 Weisz, D. R. et al. 2015, 806, 198
 Wünsch, R. et al. 2017, ApJ, 835, 60
 Yaghoobi, A. et al. 2022, MNRAS, 510, 4330
 Zonoozi, A. H., Haghi, H., Kroupa, P. 2016, ApJ, 826, 89